

# Temperature dependence of NADPH oxidase in human eosinophils

Deri Morgan, Vladimir V. Cherny, Ricardo Murphy, Wei Xu,\* Larry L. Thomas\* and Thomas E. DeCoursey

Department of Molecular Biophysics and Physiology, \*Department of Immunology/Microbiology, Rush Presbyterian St Luke's Medical Center, Chicago, IL 60612, USA

The phagocyte NADPH oxidase helps kill pathogens by producing superoxide anion,  $O_2^-$ . This enzyme is electrogenic because it translocates electrons across the membrane, generating an electron current,  $I_e$ . Using the permeabilized patch voltage-clamp technique, we studied the temperature dependence of  $I_e$  in human eosinophils stimulated by phorbol myristate acetate (PMA) from room temperature to  $>37^\circ\text{C}$ . For comparison, NADPH oxidase activity was assessed by cytochrome *c* reduction. The intrinsic temperature dependence of the assembled, functioning NADPH oxidase complex measured during rapid temperature increases to  $37^\circ\text{C}$  was surprisingly weak: the Arrhenius activation energy  $E_a$  was only  $14\text{ kcal mol}^{-1}$  ( $Q_{10}$ , 2.2). In contrast, steady-state NADPH oxidase activity was strongly temperature dependent at  $20\text{--}30^\circ\text{C}$ , with  $E_a$   $25.1\text{ kcal mol}^{-1}$  ( $Q_{10}$ , 4.2). The maximum  $I_e$  measured at  $34^\circ\text{C}$  was  $-30.5\text{ pA}$ . Above  $30^\circ\text{C}$ , the temperature dependence of both  $I_e$  and  $O_2^-$  production was less pronounced. Above  $37^\circ\text{C}$ ,  $I_e$  was inhibited reversibly. After rapid temperature increases, a secondary increase in  $I_e$  ensued, suggesting that high temperature promotes assembly of additional NADPH oxidase complexes. Evidently, about twice as many NADPH oxidase complexes are active near  $37^\circ\text{C}$  than at  $20^\circ\text{C}$ . Thus, the higher  $Q_{10}$  of steady-state  $I_e$  reflects both increased activity of each NADPH oxidase complex and preferential assembly of NADPH oxidase complexes at high temperature. In summary, NADPH oxidase activity in intact human eosinophils is maximal precisely at  $37^\circ\text{C}$ .

(Received 11 February 2003; accepted after revision 23 April 2003; first published online 16 May 2003)

**Corresponding author** T. DeCoursey: Department of Molecular Biophysics and Physiology, Rush Presbyterian St Luke's Medical Center, 1750 W. Harrison, Chicago, IL 60612, USA. Email: tdecours@rush.edu

Nicotinamide adenine dinucleotide phosphate (NADPH) oxidase is a multisubunit enzyme that catalyses the production of superoxide anion ( $O_2^-$ ) in phagocytes (reviewed by Babior, 1999). Reactive oxygen species derived from  $O_2^-$  are essential mediators of phagocyte host defense against infection. The importance of NADPH oxidase is evident in chronic granulomatous disease, in which mutations prevent enzyme function. These patients are susceptible to recurrent life-threatening infections and if untreated, chronic granulomatous disease is usually lethal. In resting cells, the components of NADPH oxidase are physically separated, with two membrane-bound and four cytosolic components (p67<sup>phox</sup>, p47<sup>phox</sup>, p40<sup>phox</sup>, and Rac, a small G protein). The two membrane-bound components, gp91<sup>phox</sup> and p22<sup>phox</sup>, called cytochrome  $b_{558}$ , coordinate two haem moieties, which together with an associated flavin adenine dinucleotide (FAD) comprise the electron pathway across the membrane. Upon stimulation by agonists such as opsonized bacteria, phorbol 12-myristate 13-acetate (PMA), or chemotactic peptides, cytosolic components are phosphorylated and assemble with cytochrome  $b_{558}$  to produce a functional enzyme complex. NADPH oxidase transports electrons

across the cell membrane and therefore is electrogenic (Henderson *et al.* 1987, 1988). Electrons extracted from intracellular NADPH are used to reduce extracellular (or intraphagosomal)  $O_2$  to  $O_2^-$ . To compensate for this charge translocation, protons are extruded through  $H^+$  channels (Henderson *et al.* 1987, 1988; DeCoursey & Cherny, 1993).

In spite of the importance of NADPH oxidase, limited information exists on its temperature dependence. Electron current generated by NADPH oxidase  $I_e$ , has been studied only at room temperature (Schrenzel *et al.* 1998; Bánfi *et al.* 1999; DeCoursey *et al.* 2000, 2001a,b, 2003; Cherny *et al.* 2001). Most studies of  $O_2^-$  release have been made at  $37^\circ\text{C}$ . All existing studies of  $O_2^-$  production by phagocytes at different temperatures are steady-state measurements (references in Table 2). Such studies cannot distinguish whether temperature affects the signalling pathway leading to NADPH oxidase activity, NADPH oxidase activity *per se*, or alterations in the rate of turnover (i.e. deactivation) of functioning NADPH oxidase complexes. By studying single cells and changing the temperature rapidly during the peak of the respiratory burst, we isolated the intrinsic

temperature dependence of the assembled and functioning NADPH oxidase complex in intact cells.

We studied human eosinophils because they exhibit a more vigorous respiratory burst than other phagocytes (DeChatelet *et al.* 1977; Yamashita *et al.* 1985; Shult *et al.* 1985; Petreccia *et al.* 1987; Yagisawa *et al.* 1996; Someya *et al.* 1997), with consequently larger  $I_c$  (Schrenzel *et al.* 1998; DeCoursey *et al.* 2001a; Cherny *et al.* 2001), and to our knowledge, the temperature dependence of NADPH oxidase in eosinophils has not been studied previously. PMA was used as a model agonist because it is widely studied, elicits the greatest  $O_2^-$  release, and in our hands activates nearly every cell. We found, unexpectedly, that steady-state NADPH oxidase activity is much more steeply temperature dependent than is the intrinsic activity of assembled NADPH oxidase complexes. This result suggests that increasing the temperature from 20°C to near 37°C promotes assembly of NADPH oxidase.

A preliminary account of this work has been presented (Cherny *et al.* 2003).

## METHODS

### Eosinophil isolation

Venous blood was drawn from healthy adult volunteers under informed written consent according to procedures approved by the Institutional Review Board of Rush Presbyterian St Luke's Medical Center and in accordance with Federal regulations. Neutrophils were isolated by density gradient centrifugation as described previously (DeCoursey *et al.* 2001a). Eosinophils were isolated from the neutrophil preparation by negative selection using anti-CD16 immunomagnetic beads (Hansel *et al.* 1991) as described previously (DeCoursey *et al.* 2001a). The eosinophils were suspended in Hepes (10 mM)-buffered HBSS (with  $Ca^{2+}$  and  $Mg^{2+}$ ), pH 7.4, containing 1 mg ml<sup>-1</sup> human serum albumin (Hepes-HBSS-HSA buffer).

### Superoxide anion production

Superoxide anion ( $O_2^-$ ) production was measured essentially as described previously (Horie & Kita, 1994; DeCoursey *et al.* 2001a). Briefly, eosinophils at  $2.5 \times 10^5$  cells ml<sup>-1</sup> were incubated with 3.2, 16 or 65 nM phorbol myristate acetate (PMA) in Hepes-HBSS-HSA buffer containing 50  $\mu$ M cytochrome *c* for 30 min at 25, 30 or 37°C. Incubations were performed in flat-bottom 96-well tissue culture plates (Costar, Acton, MA, USA) precoated with human serum albumin (Horie & Kita, 1994) in a Ceres UV900HDI microplate reader (Bio-Tek Instruments, Inc., Winooski, VT, USA), and absorbance at 550 nm was recorded at 5 min intervals. Total incubation volume was 0.2 ml. Production of  $O_2^-$  was calculated using an extinction coefficient of  $21.1 \times 10^{-3}$  M cm<sup>-1</sup> for reduced cytochrome *c* at 550 nm (Horie & Kita, 1994). Results are expressed as nmoles  $O_2^-$  per  $10^5$  cells after subtraction of spontaneous production, which was measured in the absence of PMA stimulus.

### Electrophysiology

We studied freshly isolated eosinophils as well as eosinophils maintained overnight at 37°C in RPMI 1640 medium containing 25 mM Hepes and L-glutamine (Gibco, Grand Island, NY, USA), supplemented with 10% fetal bovine serum (Bio-Whittaker,

Walkersville, MD, USA), 100 u ml<sup>-1</sup> penicillin, 100  $\mu$ g ml<sup>-1</sup> streptomycin (Sigma Chemical Co., St Louis, MO, USA), and 1 ng ml<sup>-1</sup> recombinant human GM-CSF (R & D Systems, Inc., Minneapolis, MN, USA). No difference was observed between eosinophils that were freshly isolated or incubated overnight.

For permeabilized-patch recording, the bath solution contained (mM): 50  $NH_4^+$  in the form of 25  $(NH_4)_2SO_4$ , 100 tetramethylammonium methanesulfonate (TMAMeSO<sub>3</sub>), 1 MgCl<sub>2</sub>, 5 BES buffer, 1 EGTA, and was titrated to pH 7.0 with TMAOH. Two pipette solutions were used. Both solutions contained ~500  $\mu$ g ml<sup>-1</sup> solubilized amphotericin B (~45% purity) (Sigma) and were near 300 mosmol kg<sup>-1</sup>. 'TMA<sup>+</sup> solution' was intended to isolate proton and electron currents from other ionic conductances, and contained (mM): ~100 TMAMeSO<sub>3</sub>, 25  $(NH_4)_2SO_4$ , 5 BES, 1 EGTA, 2 MgCl<sub>2</sub>, and 0.5–1.5 CaCl<sub>2</sub> at pH 7. The more physiological 'K<sup>+</sup> solution' contained ~100 KMeSO<sub>3</sub>, 25  $(NH_4)_2SO_4$ , 1 EGTA, 5 BES, and 1 MgCl<sub>2</sub> at pH 7. We did not detect any obvious outward K<sup>+</sup> currents in human eosinophils studied with 100 mM K<sup>+</sup> in the pipette solution, consistent with previous observations (Tare *et al.* 1998). Both proton and electron currents seemed similar when studied with either solution. The  $NH_4^+$  in bath and pipette solutions 'clamps'  $pH_i$  near  $pH_o$  (Grinstein *et al.* 1994; DeCoursey *et al.* 2000).

Micropipettes were pulled using a Flaming Brown automatic pipette puller (Sutter Instruments, San Rafael, CA, USA) from 7052 glass (Garner Glass Co., Claremont, CA, USA), coated with Sylgard 184 (Dow Corning Corp., Midland, MI, USA), and heat polished to a tip resistance ranging typically between 3 and 10 M $\Omega$  with TMA<sup>+</sup> and between 3 and 7 M $\Omega$  with K<sup>+</sup> pipette solutions. Electrical contact with the pipette solution was achieved by a thin sintered Ag–AgCl pellet (In Vivo Metric Systems, Healdsburg, CA, USA) attached to a Teflon-encased silver wire, or simply a chlorided silver wire. A reference electrode made from an Ag–AgCl pellet was connected to the bath through an agar bridge made with Ringer solution. The current signal from the patch clamp (EPC-7 from List Electronic, Darmstadt, Germany, or Axopatch 200B from Axon Instruments, Foster City, CA, USA) was recorded and analysed using an Indec Laboratory Data Acquisition and Display System (Indec Corporation, Sunnyvale, CA, USA) with in-house software, or pCLAMP software supplemented by Microsoft Excel and Sigmaplot (SPSS Inc., Chicago, IL, USA). Seals were formed with Ringer solution (mM: 160 NaCl, 4.5 KCl, 2 CaCl<sub>2</sub>, 1 MgCl<sub>2</sub>, 5 Hepes, pH 7.4) in the bath, and the potential zeroed after the pipette was in contact with the cell. No liquid junction potential correction was applied. Compounds such as PMA or diphenylene iodonium chloride (DPI) were introduced into the bath by complete bath changes.

### Temperature control and recording

The bath temperature was kept at 18–21°C at the start of most experiments by Peltier devices in a feedback arrangement and monitored by a resistance temperature detector element (Omega Scientific, Stamford, CT, USA) immersed in the bath. Temperature changes were transmitted to the glass recording chamber through a supporting copper plate. The Peltier-mediated temperature controllers increased the bath temperature by 10°C in ~3 min. The temperature probe was positioned as near the cell as possible. Bath temperature was monitored continuously and recorded simultaneously on a chart recorder and using in-house software or Clampex software (Axon Instruments).

During rapid temperature changes, the recorded temperature lags behind the temperature of the cell. To correct for this lag, the

recorded temperatures were corrected according to:

$$T_{\text{corrected}} = \frac{(T_1 + T_2)}{2} + \tau \left( \frac{T_2 - T_1}{t_2 - t_1} \right), \quad (1)$$

where  $T_1$  and  $T_2$  are temperatures recorded consecutively at times  $t_1$  and  $t_2$ , respectively, and  $\tau$  is the measured time constant of the probe after immersion into hot or cold water for 1.4 s. The correction shifts the  $I_e$  values measured during rapid temperature increases to higher temperatures by  $\sim 2^\circ\text{C}$  or less. Correction had only subtle effects on the  $Q_{10}$  derived from the data.

#### Calculation of $Q_{10}$ or Arrhenius activation energies

The relative change in a parameter for a  $10^\circ\text{C}$  change in temperature, the  $Q_{10}$ , was calculated by:

$$Q_{10} = \left( \frac{X_2}{X_1} \right)^{10/(T_2 - T_1)}, \quad (2)$$

where  $X_2$  is the parameter value at the higher temperature  $T_2$  and  $X_1$  is the parameter value at the lower temperature  $T_1$ . Operationally, we usually extracted  $Q_{10}$  values by plotting the data on semi-log axes, drawing a straight line through the points (by linear regression), and determining its slope. Data considered less reliable were given lower weight in this process. Arrhenius activation energies were calculated from (Kimura & Meves, 1979):

$$E_a = \frac{RT_1 T_2}{T_2 - T_1} \ln \frac{X_2}{X_1}, \quad (3)$$

where,  $R$  is the gas constant ( $8.314 \text{ J K}^{-1} \text{ mol}^{-1}$ , or  $1.9872 \text{ cal K}^{-1} \text{ mol}^{-1}$ ), and  $T_1$  and  $T_2$  are temperatures in K.

## RESULTS

### Steady-state temperature dependence of $I_e$

When activated by stimuli such as PMA, the NADPH oxidase complex in phagocytes transports electrons out of the cell, generating an inward electron current  $I_e$ , (Schrenzel *et al.* 1998; DeCoursey *et al.* 2000). In permeabilized patch configuration,  $I_e$  is detected as an increase in the inward holding current, which was measured at  $-60 \text{ mV}$ . Figure 1 shows the effects of PMA and increased temperature on membrane currents in an eosinophil. As shown by Fig. 1A (lower trace), the inward holding current began to increase shortly after addition of  $60 \text{ nM}$  PMA. Downward deflections indicate inward current, carried in this case by outward movement of electrons across the cell membrane. As the bath was routinely maintained at  $18\text{--}21^\circ\text{C}$ , which was below room temperature, changing the bath solution transiently increased the temperature (Fig. 1A, top trace). The temperature of the bath returned to its set point within a few minutes and the holding current reached a steady-state value of  $-9.5 \text{ pA}$ . Increasing the temperature to above  $30^\circ\text{C}$  caused a large increase in inward current. This PMA-induced inward current was largely abolished over  $\sim 2 \text{ min}$  by the addition of  $6 \mu\text{M}$  DPI (Fig. 1A). DPI is an inhibitor of NADPH oxidase (Robertson *et al.* 1990), thus the inward current that was activated by PMA and which increased at high temperature was  $I_e$  generated by NADPH oxidase.

During most experiments we applied depolarizing pulses at regular intervals to monitor changes in  $\text{H}^+$  and leak currents.  $\text{H}^+$  current properties change profoundly and characteristically in phagocytes treated with PMA (DeCoursey *et al.* 2000; 2001a, b), and these changes corroborate the activation of the respiratory burst inferred from the appearance of  $I_e$ . The interruptions in the holding current in Fig. 1A (lower trace) were caused by 4 s depolarizing pulses from  $-60 \text{ mV}$  to  $+40 \text{ mV}$ . In Fig. 1B, selected  $\text{H}^+$  current traces from this experiment are superimposed. Comparison of the control current (a) and currents recorded 30 s (b) and 3 min (c) after PMA stimulation reveal that PMA stimulation increases the proton current,  $I_{\text{H}}$  and results in faster activation and slower deactivation (smaller activation time constant,  $\tau_{\text{act}}$ , and larger deactivation time constant,  $\tau_{\text{tail}}$ , respectively), as described previously (DeCoursey *et al.* 2000, 2001a). The time course of the slowing of  $\tau_{\text{tail}}$  mirrored that of turn-on of  $I_e$  (Fig. 1B traces b and c).

Increasing the temperature in PMA stimulated cells (Fig. 1B traces c and d) increased  $I_{\text{H}}$  and decreased both  $\tau_{\text{act}}$  and  $\tau_{\text{tail}}$ . The temperature dependence of  $I_{\text{H}}$ ,  $\tau_{\text{act}}$ , and  $\tau_{\text{tail}}$  were similar in unstimulated and PMA-activated eosinophils (data not shown). After DPI addition (Fig. 1B, trace e),  $\tau_{\text{tail}}$  was twice as fast but there was no obvious change in  $\tau_{\text{act}}$  and no immediate change in  $I_{\text{H}}$ . DPI had no clear effect on  $I_{\text{H}}$  in most cells studied.

### Quantification of $I_e$

The inward electron current was quantified by subtracting the initial 'leak' current recorded at room temperature before the addition of PMA. The average current at  $-60 \text{ mV}$  was  $-1.8 \pm 1.3 \text{ pA}$  (mean  $\pm$  S.D.) in 53 patches studied with  $\text{K}^+$  pipette solution, similar to  $-2 \text{ pA}$  found previously with  $\text{TMA}^+$  solution (Cherny *et al.* 2001). Possible spurious effects of temperature or PMA on leak current were found to be minimal by measuring leak current at high temperature (a) in unstimulated cells, (b) after spontaneous shutdown of  $I_e$  and (c) after inhibition by DPI. The first two approaches are illustrated in Fig. 2. Increasing the temperature before PMA stimulation increased the holding (leak) current by only  $\sim 1 \text{ pA}$ . The holding current in seven unstimulated cells increased by  $2.0 \pm 0.3 \text{ pA}$  (mean  $\pm$  S.E.M.) during temperature increases from  $\sim 20^\circ\text{C}$  to  $> 30^\circ\text{C}$ . Addition of PMA at  $\sim 34^\circ\text{C}$  (Fig. 2) produced a rapid turn on of inward current, presumably  $I_e$ , which shut down spontaneously  $\sim 1 \text{ min}$  later, probably reflecting a transition to whole-cell configuration. Nevertheless, after shutdown of  $I_e$ , the holding current at  $35^\circ\text{C}$  was reduced to its value before PMA was added, indicating that the entire inward current activated by PMA and enhanced at high temperature was reversible and thus does not reflect non-specific membrane damage. The third approach (shown in Fig. 1A) was to add DPI at high temperature to inhibit NADPH oxidase activity. In several

cells, the residual DPI-insensitive 'leak' current at high temperature was similar to that obtained by the other two methods. As the increase in holding current at high temperature was small, variable, and not known in every cell, we corrected  $I_e$  only for the measured leak at low temperature. If the leak current increased by 2 pA at high temperature, for example, then the measured  $Q_{10}$  of 4.2 (Table 1) could be 'corrected' to 3.8.

### Spontaneous whole-cell configuration rapidly shuts down NADPH oxidase

In many PMA-stimulated cells, such as the one in Fig. 2,  $I_e$  suddenly decreased. We hypothesized that 'shut-down' of  $I_e$  resulted from patch rupture. The holding current typically became 'noisy' within a few minutes after

shutdown, presumably reflecting the insertion of amphotericin into the plasma membrane and resultant permeabilization of the entire cell membrane. Shortly afterwards the cell died (became very leaky). Shut-down seemed to occur preferentially at higher temperatures but did occur at room temperature in some cells, as reported previously (DeCoursey *et al.* 2001a). To confirm that spontaneous shut-down reflects rupture of the patch, we added Lucifer Yellow (a membrane impermeant fluorescent dye) to the pipette solution. No fluorescence was seen in nine cells during permeabilized patch recording for up to 20–30 min, but within ~30 s after  $I_e$  had shut down spontaneously, the cells fluoresced brightly together with the pipette, demonstrating that Lucifer Yellow dye had entered the cell (data not shown). Rapid

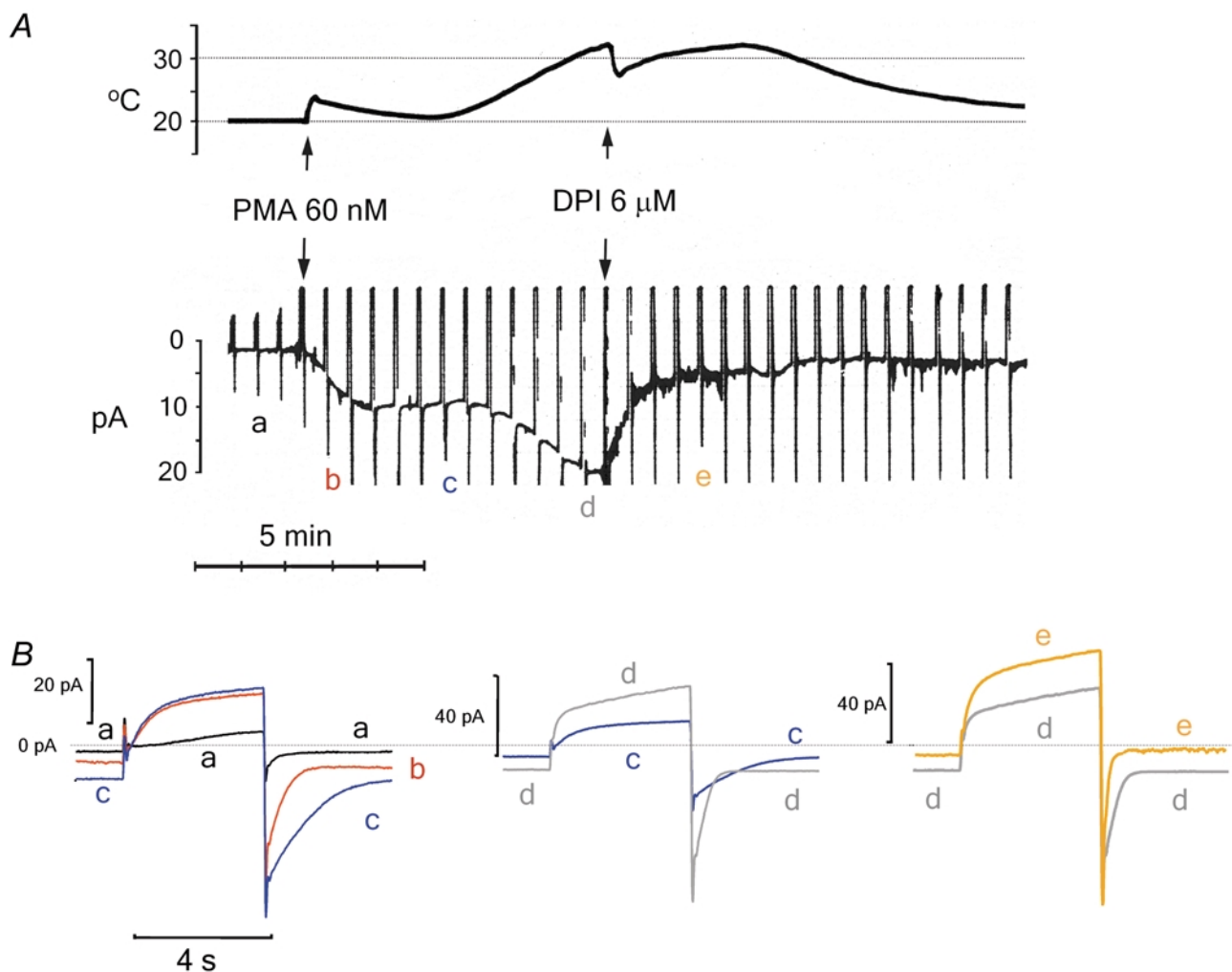


**Figure 1. Temperature dependence of PMA-stimulated  $I_e$  and  $I_H$**

A, bath temperature (top trace) and holding current (bottom trace) at  $-60$  mV were recorded simultaneously in an eosinophil in permeabilized-patch configuration. The bath and pipette contained TMA solutions. The holding current is interrupted by 4 s pulses to  $+40$  mV applied every 30 s to monitor changes in proton current. PMA and DPI were added as indicated (arrows in A). After the holding current reached a steady state the temperature was increased. B, selected  $H^+$  current records labelled in A with lower case letters, are superimposed to illustrate changes upon stimulation with PMA (a, b and c), increased temperature (c and d), and DPI (d and e), respectively. In this cell  $I_H$  was increased ~2 min after DPI addition, but some of the increase was due to removal of  $I_e$  which was inward even at the test potential,  $+40$  mV. No clear effect of DPI on the  $I_H$  amplitude was seen in most cells.

appearance of Lucifer Yellow fluorescence in the cell was seen in three cells after  $I_e$  shut down spontaneously and in three cells in which the patch was ruptured intentionally by suction. Thus, spontaneous shut down of  $I_e$  indicates patch rupture.

The rapidity of the turn-off of  $I_e$  after patch rupture was striking (Fig. 3, trace a). It is noteworthy that  $I_e$  decreased more rapidly during shut down than after inhibition with DPI (cf. Figs 1A and 3). Fit by an exponential decay function, the time constant for shut-down,  $5.6 \pm 1.8$  s (mean  $\pm$  S.E.M.  $n = 7$ ), was significantly faster than that for DPI inhibition,  $25.5 \pm 1.6$  s ( $n = 5$ ;  $P < 0.01$ , Student's  $t$  test), measured at roughly similar high temperatures. (Shut-down occurred at  $31.5 \pm 1.8^\circ\text{C}$  ( $n = 7$ ) and DPI inhibition was measured between 27 and  $30^\circ\text{C}$ .) Schrenzel *et al.* (1998) reported that  $I_e$  could be recorded in whole-cell configuration if 8 mM NADPH (the substrate for NADPH oxidase) and 1 mM ATP were included in the pipette solution. To test whether the shut-down of  $I_e$  in the present study was due to diffusion of NADPH into the pipette, we included 8 mM NADPH and 1 mM MgATP in the pipette solution. In four experiments,  $I_e$  shut down spontaneously and the residual currents were insensitive to DPI (data not shown). Thus the transition to whole-cell configuration turns off  $I_e$  by some mechanism other than diffusional loss of NADPH or ATP.

After shut-down of  $I_e$  (Fig. 3), the  $\text{H}^+$  current decreased progressively over several minutes.  $\text{H}^+$  currents that were dramatically enhanced by PMA thus revert to pre-stimulated properties (smaller  $I_{\text{H}}$  and larger  $\tau_{\text{act}}$ ) upon establishment of whole-cell configuration. The different time courses suggest that different factors maintain  $I_e$  and the activated mode of  $\text{H}^+$  channel gating.

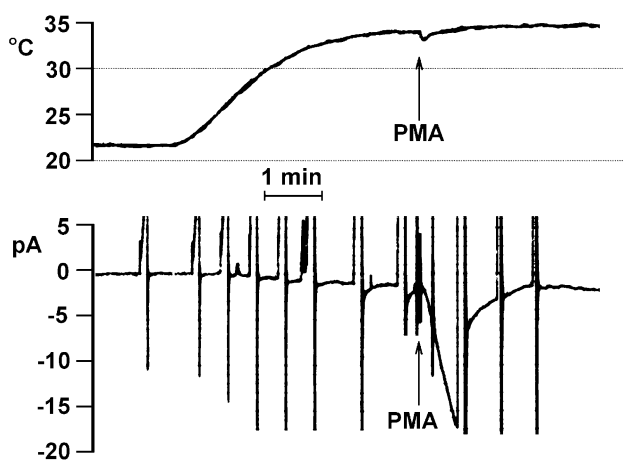


**Figure 2. Activation of  $I_e$  at high temperature**

Bath temperature (top trace) and holding current (bottom trace) at  $-60$  mV in a cell studied with  $\text{TMA}^+$  solutions. After establishing the patch, the temperature was increased to  $34^\circ\text{C}$  and PMA was added (arrow). Note that the holding (leak) current increased only  $\sim 1$  pA at high temperature.  $I_e$  shut down during a test pulse.

**Table 1. Temperature dependence of steady-state NADPH oxidase activity**

	$Q_{10}$	$E_a$ (kcal mol $^{-1}$ )
$I_e$ , $\text{K}^+$ pipette	$4.2 \pm 0.2$ (11)	$25.1 \pm 0.9$ (11)
$I_e$ , $\text{TMA}^+$ pipette	$3.4 \pm 0.3$ (13)	$21.5 \pm 1.3^*$ (13)
Superoxide	$2.8 \pm 0.3$ (4)	$17.9 \pm 2.4$ (4)

Eosinophils were stimulated with 60 nM PMA using  $\text{TMA}^+$  or  $\text{K}^+$  pipette solutions in permeabilized patch experiments.  $Q_{10}$  and  $E_a$  were calculated from linear portions of semi-logarithmic plots of  $I_e$  or the maximum rate of  $\text{O}_2^-$  production against temperature in individual experiments, which were then averaged. Data are means  $\pm$  S.E.M. of the number of cells or experiments stated in parentheses. \* $P < 0.05$   $\text{K}^+$  vs.  $\text{TMA}^+$  by Student's  $t$  test.

### Rapid temperature increases reveal weak intrinsic temperature dependence of NADPH oxidase

Like existing studies of  $\text{O}_2^-$  release at different temperatures,  $I_e$  measured during slow temperature changes (e.g. Fig. 1) does not reflect the temperature dependence of the NADPH oxidase complex directly. Instead, such measurements reflect a combination of several processes, such as protein phosphorylation, second messenger diffusion, conformational changes in NADPH oxidase components and assembly of NADPH oxidase complexes. In order to isolate the intrinsic temperature dependence of already-assembled and functioning NADPH oxidase complexes, we elicited  $I_e$  by PMA stimulation at room temperature and then increased the temperature rapidly by exchanging the bath with a pre-warmed identical PMA-containing solution (arrows in Fig. 4A). The measured bath temperature increased by  $20^\circ\text{C}$  in  $< 10$  s in the two cells illustrated in Fig. 4B (a time-

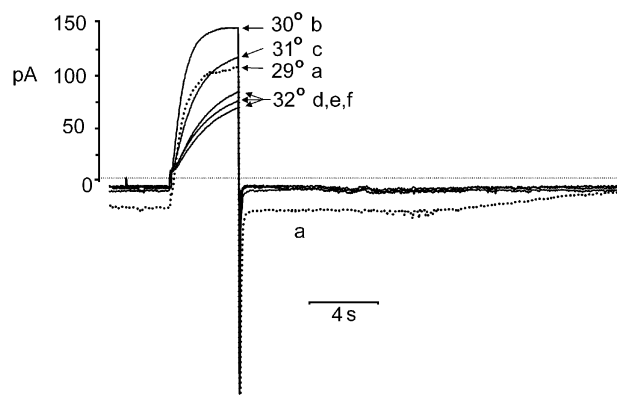


**Figure 3. Distinct time courses of changes in  $I_e$  and  $\text{H}^+$  currents in whole-cell configuration**

An eosinophil stimulated with 60 nM PMA was held at  $-60$  mV and test pulses to 40 mV were applied every 30 s; the entire 30 s epoch is shown. Sequential pulses are labelled a–f, with the approximate temperature indicated. During the first illustrated pulse epoch (a, dotted curve),  $I_e$  decreased precipitously and spontaneously. During the next 5 pulses (b–f), although the temperature continued to increase, the  $\text{H}^+$  current became progressively smaller and activated more slowly.

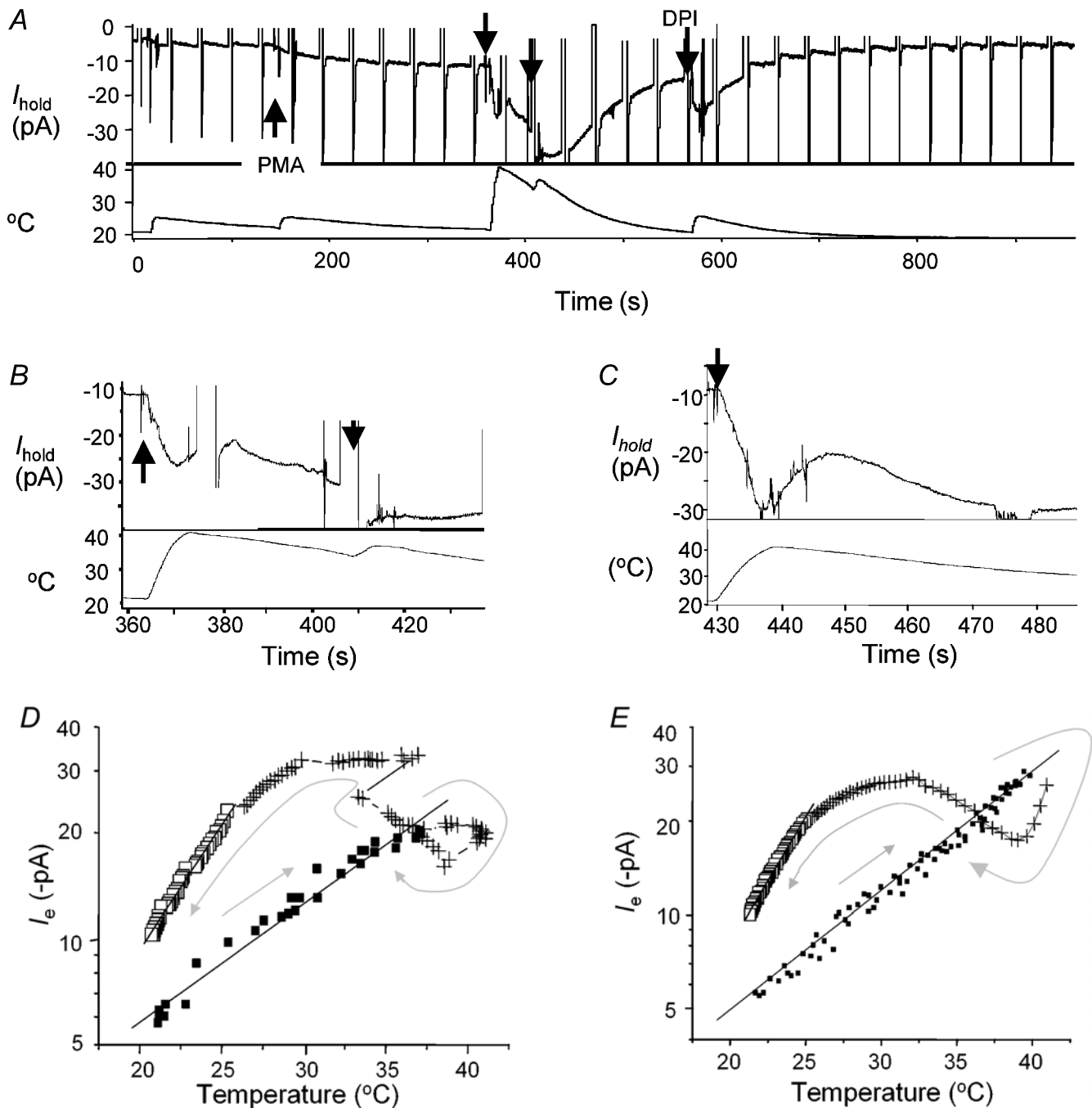


**Figure 4.**  $I_e$  during a rapid increase of temperature

*A*, electron current response to a rapid increase in temperature. An eosinophil was stimulated with PMA at room temperature and then the bath was exchanged with the same solution after pre-warming (second and third arrows). Finally DPI was added, which increased the bath temperature transiently and then reduced the holding current to near its value at the start of the experiment before PMA was added. The first transient temperature increase at  $\sim 10$  s (not labelled) was a control bath wash. *B*, shows the addition of warmed PMA from *A* on an expanded time scale. *C*, is an experiment in another cell similar to the one in *A* and *B* but without test pulses. In *D* and *E*  $I_e$  is plotted against temperature for the experiments shown in *B* and *C*, respectively. The points obtained during the initial addition of warm PMA ( $\blacksquare$ ) were used to calculate  $Q_{10}$  during rapid temperature increases, 2.16 (*D*) or 2.41 (*E*). The  $+$  show the temporal progression of complex changes that occurred at high temperatures. The  $\square$  indicate a linear region during the slow return to  $20^\circ\text{C}$ , with a slope corresponding to a  $Q_{10}$  of 5.1 (*D*) or 6.5 (*E*). Arrows show the temporal sequence of the measurements. These experiments were done with  $\text{K}^+$  pipette solutions. All data were corrected for the response time of the temperature probe (see Methods).

expanded view of Fig. 4A) and 4C. In Fig. 4D and E,  $I_e$  (after leak subtraction) is plotted against temperature in the two experiments in Fig. 4B and 4C, respectively. The  $(\log) I_e$  vs. temperature plot was linear when measured during rapid temperature increases from  $21.1 \pm 2.1$  to  $38.5 \pm 0.6^\circ\text{C}$  (mean  $\pm$  S.E.M.) in eight cells. However, the temperature dependence of  $I_e$  was surprisingly weak, the  $Q_{10}$  averaging  $2.2 \pm 0.11$  (mean  $\pm$  S.E.M.) and  $E_a$   $14.1 \pm 0.9$  kcal mol $^{-1}$ . As a result,  $I_e$  was smaller at  $37^\circ\text{C}$  after rapid temperature increases,  $-20.9 \pm 2.0$  pA, than when measured at lower temperatures during gradual temperature increases (see below).

### NADPH oxidase is inhibited at temperatures $> 37^\circ\text{C}$

During rapid temperature increases beyond  $37^\circ\text{C}$ ,  $I_e$  peaked and then decreased substantially over the next  $\sim 10$  s in both cells illustrated in Fig. 4B and C. Inhibition of  $I_e$  occurred at  $39\text{--}41^\circ\text{C}$  in similar experiments in four cells. Inhibition of  $I_e$  was not due to the rapid temperature change *per se*, but rather to acute exposure to high temperature, because inhibition was not observed in other cells after rapid increases of bath temperature to  $30\text{--}35^\circ\text{C}$ . Reduced NADPH oxidase activity in phagocytes at temperatures above  $37^\circ\text{C}$  has been described previously (Smith & Iden, 1981; Severns *et al.* 1986; Henderson, 1988; Maridonneau-Parini *et al.* 1988, 1993). The present experiments reveal the time course of high temperature-induced inhibition.

Paradoxically, after the inhibition of  $I_e$ , and while the temperature slowly decreased,  $I_e$  increased substantially over the following  $20\text{--}30$  s (Fig. 4B and C). The experiment illustrated in Fig. 4C, which was done without test pulses, clearly illustrates this secondary rise in  $I_e$ . A secondary

increase in  $I_e$  was seen in six cells, and was more pronounced when the initial bath temperature increase was more rapid (i.e. when the temperature was increased from  $\sim 20\text{--}40^\circ\text{C}$  in  $< 10$  s, rather than in  $15\text{--}20$  s). This secondary increase in  $I_e$  was entirely unexpected. After the secondary peak,  $I_e$  decreased at first gradually and then more steeply as the bath cooled. The slope during the final decrease from  $25\text{--}31$  to  $17\text{--}21^\circ\text{C}$  in four similar experiments (open squares in Fig. 4D and E) corresponded to a  $Q_{10}$  of  $6.0 \pm 0.6$  (mean  $\pm$  S.E.M.).

### Steady-state temperature dependence of PMA-stimulated $I_e$

The steady-state temperature dependence of  $I_e$  was measured during slow temperature increases (e.g. Fig. 1). Figure 5 summarizes the temperature dependence of  $I_e$  studied with TMA $^+$  or K $^+$  pipette solutions. There is remarkably little cell-to-cell scatter in the  $I_e$  measured with either solution, with all values falling within a 2–3-fold range (Fig. 5A). Examination of the individual experiments (connected by lines) in Fig. 5A reveals that  $I_e$  increased exponentially with increasing temperature (linearly on semi-logarithmic axes) between  $20$  and  $> 30^\circ\text{C}$ , but the slope decreased at higher temperatures. Arrhenius plots of the  $I_e$  data (Fig. 5B) were approximately linear over this temperature range. The  $Q_{10}$  and  $E_a$  values derived in each cell from this linear region are summarized in Table 1.

There were subtle differences between cells studied with K $^+$  and TMA $^+$  pipette solutions. The temperature dependence was slightly steeper with K $^+$  solution, although the average  $I_e$  with TMA $^+$  and K $^+$  solutions (Fig. 5B) differs significantly only above  $29^\circ\text{C}$ .  $I_e$  had a tendency to saturate, deviating from linearity typically at  $\sim 30^\circ\text{C}$  in cells studied with TMA $^+$  solution, and at  $\sim 33^\circ\text{C}$  with K $^+$  solutions. That

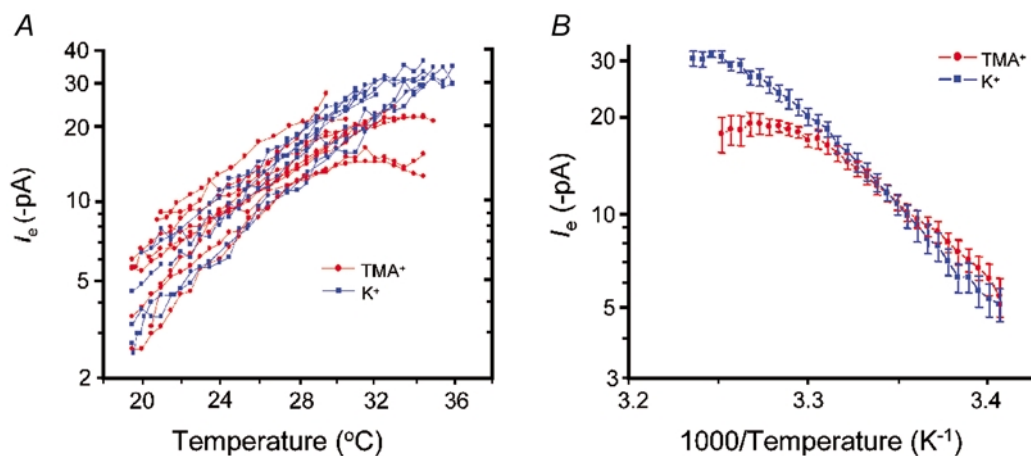


**Figure 5. Temperature dependence of  $I_e$  in eosinophils studied with TMA $^+$  or K $^+$  pipette solutions**

A,  $I_e$  in representative individual cells studied with symmetrical TMA $^+$  solutions (red  $\bullet$ ) or with K $^+$  solution in the pipette and TMA $^+$  in the bath (blue  $\blacksquare$ ) are illustrated by symbols connected with lines. B, Arrhenius plots of means  $\pm$  S.E.M.  $I_e$  from the same 11 cells studied with TMA $^+$  solution (red  $\bullet$ ) and 8 cells studied with K $^+$  solution (blue  $\blacksquare$ ) that were shown individually in A. The  $I_e$  values for TMA $^+$  and K $^+$  solutions differ significantly only above  $29^\circ\text{C}$ .

saturation was less apparent in  $K^+$  solutions suggests that part of the saturation with  $TMA^+$  solution is not intrinsic to NADPH oxidase. The maximum  $I_e$  measured directly in individual cells at high temperature (with no attempt to correct for saturation) was  $-19.8 \pm 1.2$  pA (mean  $\pm$  S.E.M.,  $n = 13$ ) at  $31.1 \pm 0.5^\circ\text{C}$  with  $TMA^+$  containing pipette solutions and  $-30.5 \pm 1.7$  pA ( $n = 12$ ) at  $33.9 \pm 0.6^\circ\text{C}$  with  $K^+$  pipette solutions.

### Superoxide anion production by eosinophils stimulated with PMA

Because  $O_2^-$  release by eosinophils has not been studied previously at different temperatures, we were curious whether the Arrhenius plot of  $O_2^-$  release would exhibit non-linearity as was observed for  $I_e$ . Eosinophil suspensions were stimulated with 65 nM PMA and reduction of cytochrome *c* was measured at 25, 30 and  $37^\circ\text{C}$  (Fig. 6A). Nearly identical results were obtained with 3.2 or 16 nM PMA (data not shown). In each of the four experiments (different symbols connected by lines in Fig. 6B), the temperature dependence of  $O_2^-$  production was weaker above  $30^\circ\text{C}$ . The mean  $Q_{10}$  was  $2.8 \pm 0.3$  between 25 and  $30^\circ\text{C}$ , but only  $1.6 \pm 0.1$  between 30 and  $37^\circ\text{C}$ . Thus, NADPH oxidase exhibits similarly weak temperature dependence above  $30^\circ\text{C}$ , whether assessed by cytochrome *c* reduction in a cuvette containing 50 000 cells or by direct measurement of  $I_e$  in individual eosinophils.

## DISCUSSION

The present study differs in four important respects from all previous studies of NADPH oxidase activity at different temperatures. First, we measured  $I_e$  generated by NADPH oxidase, rather than  $O_2^-$  generation. Second, we studied single cells, rather than populations of cells. Third, we assessed the effects of temperature changes imposed during the respiratory burst, rather than making measurements at constant temperature. Fourth, we measured NADPH oxidase activity at high temperature

in cells that were stimulated at low temperature. Consequently, the results provide novel information, some of which could not be obtained using traditional assays. The main observations are:

1. Steady-state NADPH oxidase activity is strongly temperature dependent, with a linear Arrhenius plot between  $20$ – $30^\circ\text{C}$ , and  $E_a$  of  $25$  kcal mol $^{-1}$  ( $Q_{10}$  4.2).
2. Steady-state NADPH oxidase activity is less steeply temperature dependent above  $30^\circ\text{C}$ , whether assessed as  $I_e$  or as  $O_2^-$  production.
3. After spontaneous or intentional patch rupture resulting in whole-cell configuration,  $I_e$  shuts down abruptly and  $H^+$  currents revert more gradually to their properties before PMA stimulation. Including NADPH and ATP in the pipette solution does not prevent shut-down of NADPH oxidase.
4. The Arrhenius plot of  $I_e$  measured during rapid temperature increases is linear up to  $38^\circ\text{C}$ , suggesting a single rate-limiting process, with a small  $E_a$  of  $14.1$  kcal mol $^{-1}$  ( $Q_{10}$  2.2). We consider this measurement to reflect the intrinsic temperature dependence of the assembled and functioning NADPH oxidase complex.
5. After rapid temperature increases to  $> 37^\circ\text{C}$ , there is inhibition of  $I_e$ , followed by a secondary increase in  $I_e$ . The  $I_e$  vs. temperature graph displays hysteresis, with larger  $I_e$  at each temperature as the temperature decreases than during the rapid temperature increase.

### Steady-state temperature dependence of NADPH oxidase

We consider the measurement of  $I_e$  during slow temperature changes ( $3$ – $4^\circ\text{C min}^{-1}$ ) to reflect steady-state NADPH oxidase activity. NADPH oxidase turns over at  $\sim 300$  s $^{-1}$  at  $20^\circ\text{C}$  (Koshkin *et al.* 1997; Cross *et al.* 1999c), thus, each complete electron translocation event requires at most  $\sim 3$  ms. The entire sequence of events from PMA

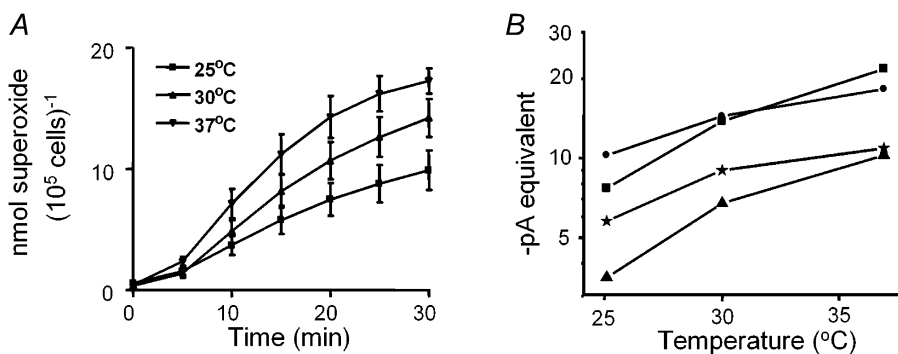


**Figure 6. Steady-state temperature dependence of superoxide production in eosinophils**

Eosinophils in suspension were stimulated with 65 nM PMA at three different temperatures for 30 min. Superoxide production was determined by measuring cytochrome *c* reduction every 5 min. A, means  $\pm$  S.E.M. cytochrome *c* reduction from four experiments at each temperature. B, the equivalent  $I_e$  per cell in each of the four experiments calculated from the maximum rate of cytochrome *c* reduction.



Table 2.  $Q_{10}$  of NADPH oxidase in various systems

Preparation	Temperature range (°C)	Duration of sample (min)	$Q_{10}$	Reference
Cytochrome $b_{558} + O_2$	2–40	—	1.80	Isogai <i>et al.</i> 1995
Cell-free system	10–24	—	1.82	Umeki & DeLisle, 1990
Cell-free system	4–23	—	1.80	Cross <i>et al.</i> 1984
Human neutrophil	25–37	2 min	2.15	Smith & Iden, 1981
Human neutrophil	25–37	Peak	1.95	Nelson <i>et al.</i> 1976
Human mononuclear cells	25–37	Peak	2.08	Nelson <i>et al.</i> 1976
Human neutrophil	15–23	Peak	3.87	Sohnle & Chusid, 1983
	23–37		1.00	
Human neutrophil	22–34	2 h	1.80	Severns <i>et al.</i> 1986
Human neutrophil cytoplasm	25–41	—	3.53	Henderson, 1988
Rat macrophage	10–24	60 min	4.31	Salman <i>et al.</i> 2000
	24–37		1.11	
Dolphin neutrophil	0–25	30 min	2.31	Itou <i>et al.</i> 2001
	25–37		1.28	
Human eosinophil $O_2^-$	25–30	5 min	2.80	Present study
	30–37		1.60	
$I_e$ , fast change	20–38.5	(<10 s)*	2.20	Present study
$I_e$ , slow change	20–33	(~3 min)*	4.2, 3.4	$K^+$ , TMA <sup>+</sup> solutions

Temperature dependence calculated from data in published studies of NADPH oxidase activity in various systems. Interpretation of measurements over long times (e.g. Severns *et al.* 1986; Itou *et al.* 2001) is complicated by evidence that  $O_2^-$  production by human neutrophils (Black *et al.* 1991) or monocytes (Nelson *et al.* 1976) is transient at 37 °C and sustained at 25 °C. For the present data, 'fast' and 'slow' refer to the rate at which the temperature was increased (see text). \* Unlike all other measurements, these were done in the same cells during the respiratory burst. Listed are the approximate times for the entire temperature change.

addition to achieving a steady-state level of  $I_e$  requires 1–2 min at room temperature (Fig. 1), and presumably occurs more rapidly at higher temperature (Fig. 2). Following rapid temperature changes,  $I_e$  continues to change slowly for ~1 min at ~37 °C (Fig. 4), as discussed below. Our measurements during slow temperature changes therefore approximate steady-state NADPH oxidase activity.

The steady-state  $I_e$  is steeply temperature sensitive. The Arrhenius plot is linear up to 33 °C with  $K^+$  pipette solution and 30 °C with TMA<sup>+</sup> pipette solution, with  $E_a$  25.1 and 21.5 kcal mol<sup>-1</sup> respectively (Table 1). These values are consistent with previous studies of  $O_2^-$  production by intact phagocytes in which both stimulation and  $O_2^-$  measurement were done at constant temperature (Table 2). The linearity of the Arrhenius plot is consistent with the idea that a single process is rate determining over this temperature range.

#### The Arrhenius plot of steady-state NADPH oxidase activity is non-linear above 30 °C

The Arrhenius plot of steady-state  $I_e$  is less steep at higher temperatures. Because saturation of  $I_e$  is less pronounced with  $K^+$  than TMA<sup>+</sup> pipette solutions, part of the saturation with TMA<sup>+</sup> solution may reflect a non-physiological mechanism, such as diffusion limitation.

However, diffusion limitation of patch current seems surprising, because much larger ion flux through the patch membrane occurs during  $H^+$  currents of several hundreds of picoamperes in the same cells. The lower slope of the steady-state Arrhenius plot at high temperature is not a result of an inability of the applied  $NH_4^+$  gradient to keep pace with the tendency of NADPH oxidase activity to lower the  $pH_i$ . Comparison of the tail current reversal potential  $V_{rev}$ , of  $H^+$  currents measured at low and high temperature did not reveal a detectable shift toward more negative voltages (change in  $V_{rev}$   $+1.8 \pm 0.7$  mV, mean  $\pm$  s.e.m.  $n = 6$ ), as would have been expected if significant cytoplasmic acidification had occurred. Thus, saturation of  $I_e$  does not reflect inhibition of NADPH oxidase by low  $pH_i$ . Virtually every study of the temperature dependence of NADPH oxidase activity indicates weaker temperature dependence at higher temperatures, both in intact cells and in cell-free systems (Table 2). Thus, the weaker temperature dependence at high temperatures appears to be 'physiological', meaning that it occurs in intact cells. Since  $K^+$  is a more physiological ion than TMA<sup>+</sup>, we consider measurements with  $K^+$  pipette solutions to reflect *in vivo* behaviour most closely. Saturation is not intrinsic to the activity of assembled NADPH oxidase complexes, because it was not seen during rapid temperature increases up to 37 °C.

### Inhibition of NADPH oxidase at high temperature

NADPH oxidase is inhibited in intact neutrophils at temperatures above 37 °C (Smith & Iden, 1981; Severns *et al.* 1986; Maridonneau-Parini *et al.* 1988, 1993). Our observation that after rapid temperature increases to > 37 °C,  $I_e$  was inhibited in a time-dependent manner demonstrates that a similar phenomenon occurs at the level of single cells. In cell-free systems NADPH oxidase has a biphasic temperature dependence, with loss of function at high temperature (Cross *et al.* 1984; Umeki & DeLisle, 1990; Erickson *et al.* 1992; Grizot *et al.* 2001), but profound inhibition occurs at much lower temperatures (~25–27 °C) (Cross *et al.* 1984; Umeki & DeLisle, 1990), perhaps due to detachment of the heme from cytochrome  $b_{558}$  above 25 °C (Cross *et al.* 1984). Inhibition at very high temperature (46 °C) has been ascribed to denaturation of the p67<sup>phox</sup> component of NADPH oxidase (Erickson *et al.* 1992). Maridonneau-Parini *et al.* (1993) speculated that assembly of NADPH oxidase above 40 °C is impaired reversibly by cytoskeleton disruption, but recovery occurred on a time scale of hours (Maridonneau-Parini *et al.* 1988). In the present study, the inhibition of  $I_e$  at 39–41 °C was reversed on a time scale of tens of seconds, which argues against wholesale denaturation or cytoskeletal disruption. On the other hand, it is unclear whether the newly functional NADPH oxidase complexes are the same ones that were inhibited at high temperature, or newly assembled complexes. In cells like the one in Fig. 4B,  $I_e$  attained a substantially higher level during the secondary increase than the initial peak value, clearly indicating assembly of additional NADPH oxidase complexes. Our observations suggest that during fever, NADPH oxidase function is impaired in individual intact eosinophils.

### NADPH oxidase activity is lost rapidly when patch rupture results in whole-cell configuration

In eosinophils at high temperature, there was a tendency of  $I_e$  to switch off spontaneously. Experiments with Lucifer Yellow in the pipette solution confirmed that shut down of  $I_e$  coincided with spontaneous patch rupture, resulting in whole-cell configuration.  $I_e$  disappeared rapidly during shut-down, with a time constant of 5.6 s, consistent with the diffusion of a small molecule like NADPH from the cytoplasm into the pipette (Pusch & Neher, 1988). However, when NADPH and ATP were included in the pipette solution, shut-down still occurred, after which no DPI-sensitive current remained. Therefore the rapid shut down of  $I_e$  in whole-cell configuration must have some other explanation. In contrast,  $I_e$  was reported in whole-cell configuration by Schrenzel *et al.* (1998) in human eosinophils studied with NADPH and ATP in the pipette solution. However, their data were obtained only during the first few minutes after achieving whole-cell configuration. Under steady-state conditions in the present study,  $I_e$  was not sustained in whole-cell configuration, even with NADPH and ATP in the pipette solution.

Presumably another molecule required for NADPH oxidase activity diffuses out of the cell.

After shutdown of  $I_e$ , the  $H^+$  channel properties reverted progressively (over several min) to those in unstimulated cells (slower  $\tau_{act}$ , smaller  $I_H$ , and faster  $\tau_{tail}$ ). This phenomenon demonstrates that the activation of  $H^+$  channels by PMA is reversible, but occurs with a distinctly slower time course than the loss of  $I_e$ . Although voltage-gated proton channels and NADPH oxidase are closely related and both are activated by various respiratory burst agonists, they are functionally distinct entities (DeCoursey *et al.* 2001b; Morgan *et al.* 2002). The reversal of  $H^+$  channel properties suggests that a diffusible substance in the cytoplasm keeps  $H^+$  channels in their 'activated' gating mode. One possibility is arachidonic acid, which can reversibly alter the properties of  $H^+$  channels (DeCoursey & Cherny, 1993; Gordienko *et al.* 1996), although its effects do not perfectly mimic those of PMA (Cherny *et al.* 2001). This question deserves further investigation.

### What is $I_e$ in a human eosinophil at 37 °C?

The maximum  $I_e$  measured here at high temperature was –30.5 pA (on average at 33.9 °C) with the  $K^+$  pipette solution. This value may be considered a lower limit, because saturation of  $I_e$  might occur to a lesser extent *in vivo*. However, most studies of NADPH oxidase activity indicate a tendency toward saturation or loss of function at high temperatures (Smith & Iden, 1981; Sohnle & Chusid, 1983; Johansen *et al.* 1983; Cross *et al.* 1984; Severns *et al.* 1986; Henderson, 1988; Maridonneau-Parini *et al.* 1988; Umeki & DeLisle, 1990; Erickson *et al.* 1992; Grizot *et al.* 2001). The highest  $I_e$  equivalents derived from studies of superoxide production stimulated by PMA in intact human eosinophils at 37 °C are –34.7 pA (Tare *et al.* 1998) or –41.4 pA (Yagisawa *et al.* 1996).

Studied under our conditions,  $I_e$  might be larger than in intact cells, because the voltage-clamp artificially keeps the membrane potential at –60 mV. NADPH oxidase activity tends to cause membrane depolarization that may reach +58 mV in human neutrophils (Jankowski & Grinstein, 1999). As electron transport through NADPH oxidase complex is electrogenic, it is sensitive to membrane potential and should be inhibited by depolarization. However, we recently measured the voltage dependence of  $I_e$  in eosinophils, and found that NADPH oxidase activity is surprisingly voltage independent from –100 mV to roughly +50 mV, and therefore  $I_e$  in an intact cell would be inhibited only slightly by the depolarization that occurs during the respiratory burst (DeCoursey *et al.* 2003).

### High temperature promotes assembly of NADPH oxidase complexes

Some evidence suggests that NADPH oxidase complexes remain active only for a limited time and that sustained respiratory burst activity requires continual assembly of

new NADPH oxidase complexes (Quinn *et al.* 1993; Cross *et al.* 1999b). In addition, the mechanism by which NADPH oxidase activity is terminated is unclear (Babior, 1999). Thus, steady-state NADPH oxidase activity reflects many processes that occur in the series of events leading to NADPH oxidase activation and assembly (phosphorylation, translocation of the cytosolic components to the membrane, etc.), perhaps balanced by disassembly and/or deactivation. The linearity of the Arrhenius plot of steady-state  $I_e$  from 20 to 33 °C suggests that a single process is rate determining in this range.

The complex response of  $I_e$  to rapid temperature changes can be explained if we hypothesize that high temperature promotes the assembly of NADPH oxidase complexes in PMA-stimulated eosinophils. During a temperature increase that is too rapid to allow assembly of new NADPH oxidase complexes, those complexes that are already assembled and functional simply increase their turnover rate. The  $Q_{10}$  of  $I_e$  obtained during rapid temperature increases was only 2.2, which we take to reflect the intrinsic temperature dependence of the assembled NADPH oxidase complex. This interpretation is in agreement with the results obtained in a cell-free system (Table 2) in which the activation and assembly steps are bypassed (Cross *et al.* 1984) and in a system of purified cytochrome  $b_{558}$  reacting directly with  $O_2$  (Isogai *et al.* 1995). After rapid temperature increases, there was a delayed, secondary increase in  $I_e$ . The final  $I_e$  at high temperature, compared with the initial  $I_e$  at lower temperature gives a  $Q_{10}$  near 4, as was seen during slow temperature increases. Existing data on the temperature dependence of NADPH oxidase activity in intact cells (Table 2) are steady-state measurements at constant temperature, and thus their agreement with measurements of  $I_e$  during slow temperature increases at comparable temperatures is not surprising.

The secondary increase in  $I_e$  at high temperature presumably reflects a process leading to or involved in the assembly of additional NADPH oxidase complexes. Hysteresis of the  $I_e$  vs. temperature plot (Fig. 4D and E) indicates that twice as many NADPH oxidase complexes are active at each temperature 'on the way down' after several minutes at high temperature. Evidently, high temperature promotes assembly of a greater number of NADPH oxidase complexes than in the steady state at lower temperatures. An alternative that cannot be ruled out entirely is that high temperature promotes a state of more efficient function of each individual NADPH oxidase complex. High and intermediate modes of NADPH oxidase activity have been proposed (Cross, 1999a). However, such a mechanism would have to operate on a much slower time scale than the turnover time of electron transport. Furthermore, using an entirely different approach, Cohen *et al.* (1980) concluded that

three times as many NADPH oxidase complexes were active at 37 °C than at 25 °C. Together with existing data in intact cells and cell-free systems, our results demonstrate that NADPH oxidase in intact eosinophils operates optimally precisely at body temperature.

## REFERENCES

- Babior BM (1999). NADPH oxidase: an update. *Blood* **93**, 1464–1476.
- Bánfi B, Schrenzel J, Nüsse O, Lew DP, Ligeti E, Krause KH & Demaurex N (1999). A novel  $H^+$  conductance in eosinophils: unique characteristics and absence in chronic granulomatous disease. *J Exp Med* **190**, 183–194.
- Black CDV, Cook JA, Russo A & Samuni A (1991). Superoxide production by stimulated neutrophils: temperature effect. *Free Radic Res Commms* **12**, 27–37.
- Cohen HJ, Chovaniec ME & Davies WA (1980). Activation of the guinea pig granulocyte NAD(P)H-dependent superoxide generating enzyme: localization in a plasma membrane enriched particle and kinetics of activation. *Blood* **55**, 355–363.
- Cherny VV, Henderson LM, Xu W, Thomas LL & DeCoursey TE (2001). Activation of NADPH oxidase-related proton and electron currents in human eosinophils by arachidonic acid. *J Physiol* **535**, 783–794.
- Cherny VV, Morgan D, Xu W, Thomas LL & DeCoursey TE (2003). Complex temperature dependence of electron current generated by the phagocyte NADPH oxidase. *Biophys J* **84**, 456a.
- Cross AR, Erickson RW & Curnutte JT (1999a). Simultaneous presence of p47<sup>phox</sup> and flavocytochrome  $b_{245}$  are required for the activation of NADPH oxidase by anionic amphiphiles: evidence for an intermediate state of oxidase activation. *J Biol Chem* **274**, 15519–15525.
- Cross AR, Erickson RW & Curnutte JT (1999b). The mechanism of activation of NADPH oxidase in the cell-free system: the activation process is primarily catalytic and not through the formation of a stoichiometric complex. *Biochem J* **341**, 251–255.
- Cross AR, Erickson RW, Ellis BA & Curnutte JT (1999c). Spontaneous activation of NADPH oxidase in a cell-free system: unexpected multiple effects of magnesium ion concentrations. *Biochem J* **338**, 229–233.
- Cross AR, Parkinson JF & Jones OTG (1984). The superoxide-generating oxidase of leukocytes: NADPH-dependent reduction of flavin and cytochrome  $b$  in solubilized preparations. *Biochem J* **223**, 337–344.
- DeChatelet LR, Shirley PS, McPhail LC, Huntley CC, Muss HB & Bass DA (1977). Oxidative metabolism of the human eosinophil. *Blood* **50**, 525–535.
- DeCoursey TE & Cherny VV (1993). Potential, pH, and arachidonate gate hydrogen ion currents in human neutrophils. *Biophys J* **65**, 1590–1598.
- DeCoursey TE, Cherny VV, DeCoursey AG, Xu W & Thomas LL (2001a). Interactions between NADPH oxidase-related proton and electron currents in human eosinophils. *J Physiol* **535**, 767–781.
- DeCoursey TE, Cherny VV, Morgan D, Katz BZ & Dinauer MC (2001b). The gp91<sup>phox</sup> component of NADPH oxidase is not the voltage-gated proton channel in phagocytes, but it helps. *J Biol Chem* **276**, 36063–36066.
- DeCoursey TE, Cherny VV, Zhou W & Thomas LL (2000). Simultaneous activation of NADPH oxidase-related proton and electron currents in human neutrophils. *Proc Natl Acad Sci U S A* **97**, 6885–6889.

- DeCoursey TE, Morgan D & Cherny VV (2003). The voltage dependence of NADPH oxidase reveals why phagocytes need proton channels. *Nature* **422**, 531–534.
- Erickson RW, Malawista SE, Garrett MC, Van Blaricom G, Leto TL & Curnutte JT (1992). Identification of a thermolabile component of the human neutrophil NADPH oxidase. A model for chronic granulomatous disease caused by deficiency of the p67-*phox* cytosolic component. *J Clin Invest* **89**, 1587–1595.
- Gordienko DV, Tare M, Parveen S, Fenech CJ, Robinson C & Bolton TB (1996). Voltage-activated proton current in eosinophils from human blood. *J Physiol* **496**, 299–316.
- Grinstein S, Romanek R & Rotstein OD (1994). Method for manipulation of cytosolic pH in cells clamped in the whole cell or perforated-patch configurations. *Am J Physiol* **267**, C1152–1159.
- Grizot S, Fieschi F, Dagher MC & Pebay-Peyroula E (2001). The active N-terminal region of p67<sup>phox</sup>. Structure at 1.8 Å resolution and biochemical characterizations of the A128V mutant implicated in chronic granulomatous disease. *J Biol Chem* **276**, 21627–21631.
- Hansel TT, De Vries IJM, Iff T, Rihs S, Wandzilak M, Betz S, Blaser K & Walker C (1991). An improved immunomagnetic procedure for the isolation of highly purified human blood eosinophils. *J Immunol Methods* **145**, 105–110.
- Henderson LM (1988). The electrogenic nature of the NADPH oxidase of human neutrophils. PhD Thesis, University of Bristol, UK.
- Henderson LM, Chappell JB & Jones OTG (1987). The superoxide-generating NADPH oxidase of human neutrophils is electrogenic and associated with an H<sup>+</sup> channel. *Biochem J* **246**, 325–329.
- Henderson LM, Chappell JB & Jones OTG (1988). Superoxide generation by the electrogenic NADPH oxidase of human neutrophils is limited by the movement of a compensating charge. *Biochem J* **255**, 285–290.
- Horie S & Kita H (1994). CD11b/CD18 (Mac-1) is required for degranulation of human eosinophils induced by human recombinant granulocyte-macrophage colony-stimulating factor and platelet-activating factor. *J Immunol* **152**, 5457–5467.
- Isogai Y, Iizuka T & Shiro Y (1995). The mechanism of electron donation to molecular oxygen by phagocytic cytochrome b<sub>558</sub>. *J Biol Chem* **270**, 7853–7857.
- Itou T, Sugisawa H, Inoue Y, Jinbo T & Sakai T (2001). Oxygen radical generation and expression of NADPH oxidase genes in bottlenose dolphin (*Tursiops truncatus*) neutrophils. *Dev Comp Immunol* **25**, 47–53.
- Jankowski A & Grinstein S (1999). A noninvasive fluorimetric procedure for measurement of membrane potential. *J Biol Chem* **274**, 26098–26104.
- Johansen KS, Berger EM & Repine JE (1983). Effect of temperature on polymorphonuclear leukocyte function. *Acta Pathol Microbiol Immunol Scand Sect C* **91**, 355–359.
- Kimura JE & Meves H (1979). The effect of temperature on the asymmetrical charge movement in squid giant axons. *J Physiol* **289**, 479–500.
- Koshkin V, Lotan O & Pick E (1997). Electron transfer in the superoxide-generating NADPH oxidase complex reconstituted in vitro. *Biochim Biophys Acta* **1319**, 139–146.
- Maridonneau-Parini I, Clerc J & Polla BS (1988). Heat shock inhibits NADPH oxidase in human neutrophils. *Biochem Biophys Res Commun* **154**, 179–186.
- Maridonneau-Parini I, Malawista SE, Stubbe H, Russo-Marie F & Polla BS (1993). Heat shock in human neutrophils: superoxide generation is inhibited by a mechanism distinct from heat-denaturation of NADPH oxidase and is protected by heat shock proteins in thermotolerant cells. *J Cell Physiol* **156**, 204–211.
- Morgan D, Cherny VV, Price MO, Dinauer MC & DeCoursey TE (2002). Absence of proton channels in COS-7 cells expressing functional NADPH oxidase components. *J Gen Physiol* **119**, 571–580.
- Nelson RD, Mills EL, Simmons RL & Quie PG (1976). Chemiluminescence response of phagocytizing human monocytes. *Infect Immun* **14**, 129–134.
- Petreccia DC, Nauseef WM & Clark RA (1987). Respiratory burst of normal human eosinophils. *J Leukocyte Biol* **41**, 283–288.
- Pusch M & Neher E (1988). Rates of diffusional exchange between small cells and a measuring patch pipette. *Pflugers Arch* **411**, 204–211.
- Quinn MT, Evans T, Loetterle LR, Jesaitis AJ & Bokoch GM (1993). Translocation of Rac correlates with NADPH oxidase activation: evidence for equimolar translocation of oxidase components. *J Biol Chem* **268**, 20983–20987.
- Robertson AK, Cross AR, Jones OTG & Andrew PW (1990). The use of diphenylene iodonium, an inhibitor of NADPH oxidase, to investigate the antimicrobial action of human monocyte derived macrophages. *J Immunol Methods* **133**, 175–179.
- Salman H, Bergman M, Bessler H, Alexandrova S & Djaldetti M (2000). Ultrastructure and phagocytic activity of rat peritoneal macrophages exposed to low temperatures *in vitro*. *Cryobiology* **41**, 66–71.
- Schrenzel J, Serrander L, Bánfi B, Nüsse O, Fouyouzi R, Lew DP, Demaurex N & Krause KH (1998). Electron currents generated by the human phagocyte NADPH oxidase. *Nature* **392**, 734–737.
- Severns C, Collins-Lech C & Sohnle PG (1986). Effect of temperature on production of hypochlorous acid by stimulated human neutrophils. *J Lab Clin Med* **107**, 29–35.
- Shult PA, Graziano FM, Wallow IH & Busse WW (1985). Comparison of superoxide generation and luminol-dependent chemiluminescence with eosinophils and neutrophils from normal individuals. *J Lab Clin Med* **106**, 638–645.
- Smith RJ & Iden SS (1981). Properties of calcium ionophore-induced generation of superoxide anion by human neutrophils. *Inflammation* **5**, 177–192.
- Sohnle PG & Chusid MJ (1983). The effect of temperature on the chemiluminescence response of neutrophils from rainbow trout and man. *J Comp Pathol* **93**, 493–497.
- Someya A, Nishijima K, Nunoi H, Irie S & Nagaoka I (1997). Study on the superoxide-producing enzyme of eosinophils and neutrophils- comparison of the NADPH oxidase components. *Arch Biochem Biophys* **345**, 207–213.
- Tare M, Prestwich SA, Gordienko DV, Parveen S, Carver JE, Robinson C & Bolton TB (1998). Inwardly rectifying whole cell potassium current in human blood eosinophils. *J Physiol* **506**, 303–318.
- Umeki S & DeLisle DM (1990). A microtechnique for neutrophil respiratory burst oxidase in a cell-free system – characterization of oxidase activation system. *Comp Biochem Physiol B* **96**, 461–464.
- Yagisawa M, Yuo A, Yonemaru M, Imajoh-Ohmi S, Kanegasaki S, Yazaki Y & Takaku F (1996). Superoxide release and NADPH oxidase components in mature human phagocytes: correlation between functional capacity and amount of functional proteins. *Biochem Biophys Res Commun* **228**, 510–516.
- Yamashita T, Someya A & Hara E (1985). Response of superoxide anion production by guinea pig eosinophils to various soluble stimuli: comparison to neutrophils. *Arch Biochem Biophys* **241**, 447–452.

#### Acknowledgements

This work was supported in part by the Heart, Lung and Blood Institute of the National Institutes of Health (research grants HL52671 and HL61437 to T.E. DeCoursey) and AI48160 to L. L. Thomas. The authors appreciate the able technical assistance of Tatiana Iastrebova and Julie Murphy.